Prediction-aided Radio-interferometric Object Tracking

Gergely Zachár and Gyula Simon
Department of Computer Science and Systems Technology, University of Pannonia, Veszprém, Hungary

Keywords: Sensor Network, Localization, Tracking, Radio-interferometry, Prediction.

Abstract: In this paper a novel robust radio-interferometric object tracking method is proposed. The system contains fixed infrastructure transmitter nodes generating interference signals, the phases of which are measured by the tracked receivers and other fixed infrastructure nodes. From the measured phase values a confidence map is computed, which is used to generate the track of the moving receivers. The proposed method enhances the track estimation by an adaptive evaluation method of the confidence map, and also provides more robust estimation by allowing bad or missing measurements, which are tolerated by predictions extracted from the evolution of the confidence map in time. The performance of the proposed system is illustrated by real measurements.

1 INTRODUCTION

Object localization and tracking, where the goal is to determine the location of a target of interests, is a key service in many applications. Several different technologies have been proposed, the most notables being the image-, acoustic-, and RF-based solutions.

Image-based techniques identify image features in consecutive video frames and thus can localize and track objects (e.g. Se, 2001). Low-cost solutions use special graphical markers to aid localization (e.g. in museums (Mulloni, 2009). Other systems use a large database of pictures to determine the current location by comparing the picture taken at the unknown location to the pictures stored in the database (Kai, 2009).

Acoustic localization methods mainly use triangulation based on ranging, which is performed by measuring the time of flight of sound (Peng, 2007).

The most widespread RF-based solution is GPS, which utilizes the time of flight of electromagnetic signals emitted from several satellites to triangulate the position of a receiver. GPS can be used mainly in outdoors applications, where the line of sight to some satellites can be provided. Indoors applications also use RF-based solutions, either using received signal strength (RSSI) or the time of flight. Since RSSI cannot be used reliably for ranging (i.e. for distant measurement), RSSI-based solutions often use reference maps, measured during system setup (Au, 2012). RF ranging-based solutions measure the time of flight of RF signals, using more sophisticated hardware (Lanzisera 2011). A completely different approach was proposed in (Maroti, 2005) to avoid high frequency processing, based on radio interferometric phase measurements. The robustness and the processing speed of the radio interferometric localization were improved in (Dil, 2011) with a stochastic approach. For real-time interferometric tracking a confidence map-based approach was proposed by (Zachár, 2014), which is either able to follow the trajectory of an object if its original position is known, or it can determine the full track of a moving object retrospectively if the object has covered a sufficiently large trajectory.

In this paper a novel object tracking method will be proposed, which utilizes radio-interferometric phase measurements and confidence maps, similar to (Zachár, 2014), but enhances the robustness and quality of the position estimation. The main contributions of the paper are the following:

- For the evaluation of peaks in the confidence map a dynamic threshold value is proposed, which is based on the statistical properties of the confidence map. This solution provides more robust estimates in real situations, when the environment changes (e.g. people are moving around the tracked object).
- Missing or bad measurements are tolerated by a novel prediction method, which examines the evolution of the confidence map in time and

Zachár G. and Simon G..
Prediction-aided Radio-interferometric Object Tracking.
DOI: 10.5220/0005241501610168
In *Proceedings of the 4th International Conference on Sensor Networks* (SENSORNETS-2015), pages 161-168
ISBN: 978-989-758-086-4

extracts prediction information from it.
The proposed method provides more robust and more accurate estimates when bad measurements are present or measurements are temporarily missing. The complexity of the proposed algorithm is moderate thus it can be implemented in real time on ordinary computers.

2 RELATED WORK

The proposed solution presented in this paper strongly related to the Radio Interferometric Positioning (Maroti, 2005) in terms of the radio-interferometric measurement process and enhances the capabilities and robustness of the Radio-Interferometric Object Trajectory Estimation presented by (Zachár, 2014).

2.1 Radio Interferometric Positioning

In Radio Interferometric Positioning (RIPS) (Maroti, 2005) low cost, of the shelf components and simple signal processing methods are utilized, allowing the creation of an inexpensive positioning system in sensor networks. The basic scenario of the radio-interferometric measurement process can be seen in Figure 1. In RIPS two devices (A and B) are used for generating the interference signal by transmitting carrier signals (sine waves) with almost the same frequency (f_A and f_b). If the two frequencies are close to each other than the produced interference signal has a low frequency envelope signal with a frequency of $\Delta f = |f_A - f_B|$ at the two receivers (C and D), but the phase depends on the relative positions of the four devices. This phase difference is utilized to provide location estimates.

Note that the envelope signal of the generated interference is actually the received signal strength (RSSI), which can be determined with most RF transceivers. The phase difference ϑ between the RSSI signals can be measured if the two receivers (C and D) are time synchronized. The measurement using 4 devices and producing a phase difference value ϑ is called quad-ranging.

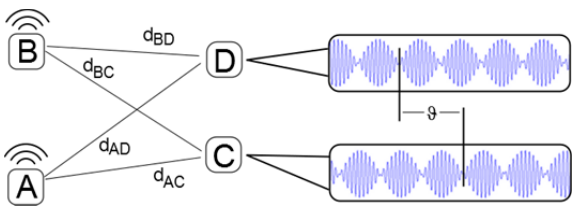

Figure 1: Radio interferometric measurements.

The phase difference ϑ depends on the relative positions of the transimtters and receivers and can be expressed as the function of the linear combination d_{ABCD} of the pairwise distances d_{AC}, d_{AD}, d_{BC}, and d_{BD} :

$$\vartheta(\lambda) = 2\pi \frac{d_{ABCD}}{\lambda} \ (mod\ 2\pi) \qquad (1)$$

where d_{AC}, d_{AD}, d_{BC}, and d_{BD} are defined in Figure 1, $d_{ABCD} = d_{AD} - d_{BD} + d_{BC} - d_{AC}$, and λ is the wavelength of the carrier frequency ($\lambda \approx \lambda_A \approx \lambda_B$). Notice that the phase values in (1) are wrapped ($0 \leq \vartheta < 2\pi$) and thus from (1) the exact value of d_{ABCD} cannot be determined, causing ambiguities in the solution. Thus one quad-ranging provides only information about a possible set of d_{ABCD} values. Performing multiple quad-ranging (using different set of measurement nodes, different frequencies, or the combination of both) enough information can be gathered to determine the unknown node location. In (Maroti, 2005) problem was addressed by solving Diophantine equations of $\vartheta(\lambda)$, using multiple carrier frequencies. The position estimates of the transmitters and receivers were determined with optimization techniques, based on a larger set of devices and multiple measurements. The main drawback of RIPS is the required high accuracy of the phase measurement. Note that the phase difference measurements on multiple frequencies are highly time consuming; in (Maroti, 2005) 80 minutes of data collection time was reported. A stochastic radio interferometric localization approach (SRIPS) were proposed in (Dil, 2011), which significantly reduces the required measurement and process time, utilizing 2.4 GHz radio transceivers, infrastructure nodes, and a stochastic positioning algorithm. SRIPS requires several quad-range measurements on different frequencies, thus it is unable to localize a moving object.

2.2 Measurement Scheduling

For radio interferometry based applications multiple quad-ranging must be performed with different sets of four devices to localize or track a device. In a given time slice only two selected transmitter devices are generating the interference signal and the other nodes are measuring the phase values in (1). The roles of the nodes are changed/alternated in time, using a measurement schedule, as was proposed in (Zachár, 2014). As an illustration, the possible schedule of four fixed infrastructure nodes (A, B, C, D) and one moving node (X) is shown in

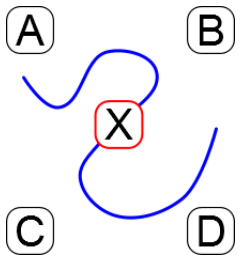

Config	A	B	C	D	X
C1	T	T	R		R
C2	T	R	T		R
C3	T	R		T	R
C4	R	T	T		R
C5	R	T		T	R
C6	R		T	T	R
C7	T	T		R	R
…					
C12		R	T	T	R

Figure 2: Possible configurations for an infrastructure, with four infrastructure nodes (A, B, C, D) and one tracked node (X).

Figure 2. The schedule contains 12 different configurations, each with 2 transmitters and 2 receivers. Note the moving node is always a receiver in each configuration, while the other roles are changing, as shown in Figure 2. Note that configurations *C1-6* and *C7-12* are identical except for the fixed reference receiver, which causes only a constant bias between the two measured phase differences in (1).

Note that the number of configurations and the required time for a measurement round remain constant with the increasing number of tracked nodes because the tracked nodes are receivers only. With more configurations the tracking robustness and accuracy can be increased.

Note that the experimental results in (Maroti, 2005) show that for radio interferometric localization or tracking the maximum distance between the transmitter and the receiver can be larger than the range of the digital communication. In our experimental tests the devices used for quad-range measurement must be in the range of the digital communication due to the utilized time synchronization, resulting a range of a few dozens of meters.

2.3 Interferometric Tracking

In (Zachár, 2014) a novel method was proposed where the positioning and tracking is performed in a different way; instead of directly calculating the position estimator (e.g. as in (Maroti, 2005)) an intermediate confidence map $\beta(p,k) = 1 - \varepsilon(p,k)$ is computed for the entire measurement area, with the following error function:

$$\varepsilon(p,k) = \frac{1}{C\pi^2}\sum_{c=1}^{C}\left(\Delta\vartheta_c(p,k)\right)^2 \qquad (2)$$

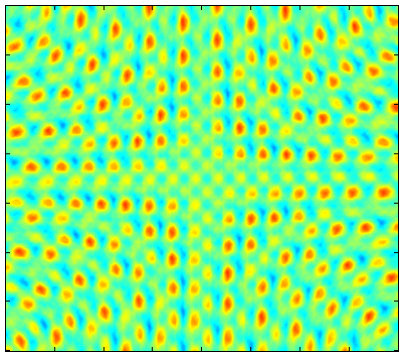

Figure 3: Confidence map, measured and calculated by a measurement setup similar to one in Figure 2.

where p is the position under calculation and k is the measurement round, producing C measurements for each c configuration, as follows:

$$\vartheta_{meas}(k) = [\vartheta_1(k), \vartheta_2(k), \ldots, \vartheta_C(k)] \qquad (3)$$

and $\Delta\vartheta_c$ represents the difference between the ideal and the measured phase difference values:

$$\Delta\vartheta_c(p,k) = \min_{i=-1,0,1}\left|\vartheta_c^{(id)}(p) + i2\pi - \vartheta_c(k)\right| \qquad (4)$$

The resulting 2D confidence map shown in Figure 3. contains several peaks which represent the possible positions of the object. This provides a possibility to locate and track all of the possible locations simultaneously with low computation cost thus make the tracking feasible in real time.

The map in Figure 3 contains a peak, corresponding to the true position of the tracked device, and phantom positions. As the object moves, the peaks are also moving in the confidence map. Once the initial position of the object is known, the tracking problem can trivially be translated into the problem of following the position of the peak, corresponding to the true location, in the confidence map. The method proposed in (Zachár, 2014), however, goes further and determines the track of a moving object, even if the initial position is not known.

The method in (Zachár, 2014) is based upon the behavior of the peaks in the confidence map: the confidence value of the peak, which belongs to the

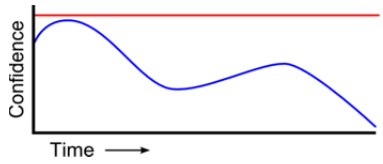

Figure 4: Illustration of the ideal confidence values corresponding to the true trajectory (red) and a phantom trajectory (blue).

true position remains constantly high (illustrated by a red curve in Figure 4), but the confidence values belonging to phantom positions fluctuate heavily and eventually disappear (blue curve in Figure 4), as the object is moving. This feature of the confidence map makes it possible to distinguish between the phantom tracks and the real track of the object over time. The proposed algorithm in (Zachár, 2014) tracks all of the possible positions as long as the corresponding peaks in the confidence map are high, and disposes those phantom tracks, where the peak value decreases below a limit, thus after a sufficiently long track only the true trajectory remains.

Unfortunately the algorithm of (Zachár, 2014) lacks the possibility to continue a track if a peak is disappearing for a few measurement rounds due to e.g. erroneous or missing phase measurements or faulty peak detection on the confidence map. In practical situations bad measurements are present, measurement results may be lost due to communication problems, and in such cases the track may be lost. In this paper two means are proposed to avoid such problems, thus to provide more robust trajectory estimates.

3 PROPOSED SOLUTION

The proposed solution provides an enhanced and more robust tracking method based on a confidence map. The proposed techniques are illustrated in Figure 5. The original method of (Zachár, 2014) uses a fixed threshold. As opposed to the ideal case, illustrated in Figure 4, real measurements often results in true peaks with smaller amplitude, thus the original method may lose tracks, as illustrated in Figure 5(a). The proposed adaptive peak search method, illustrated in Figure 5(b) and discussed in Section 3.1, uses an adaptive threshold, thus the number of peak losses can be decreased (but not necessarily fully prevented). The peaks, which are lost for a short time, would result in complete track loss, which is prevented by the proposed prediction method, described in Section 3.2: if a track seems to end, due to the lost peak, the track it is maintained for a while, using predicted peaks from neighborhood information. Thus temporary peak losses can be tolerated, as illustrated in Figure 5(c).

The new tracking algorithm, using adaptive threshold and predictive track enhancement is formalized in Section 3.3.

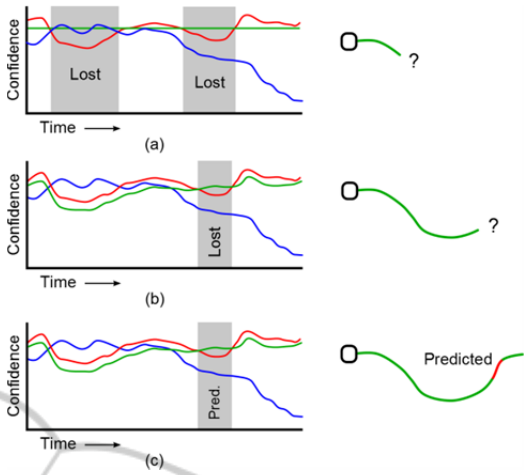

Figure 5: Left column: confidence values of real objects (red), phantom objects (blue) and the thresholds (green); Right column: estimated object trajectories. (a) constant threshold, with two peak-losses, resulting in a track loss, (b) adaptive threshold, still peak loss possible, causing track loss, (c) adaptive threshold with prediction, which tolerates temporary peak losses.

3.1 Adaptive Peak Extraction

The proposed object tracking algorithm operates on the possible positions, extracted from the peaks of the confidence map in each measurement round, thus the quality of the peak extraction heavily influences the accuracy and robustness of the tracking. In the case of noisy measurements the confidence map can be blurred and may contain multiple smaller peaks rather than one, sharp peak in a possible position. The proposed solution uses binarization with an adaptive threshold.

The proposed peak extraction is illustrated in Figure 6. The algorithm uses the confidence map, as input (see Figure 6(a)). In the first step high peaks are selected using the threshold, resulting a new binary map where peaks higher than the threshold are represented as blobs, as shown in Figure 6(b). In the second step, shown in Figure 6(c), possible positions are determined as the geometric centers of each region, thus eliminating the issues with blurred or multiple peaks.

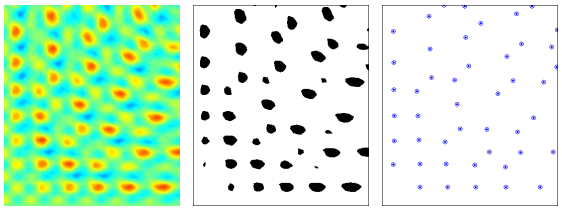

Figure 6: Peak extraction. (a) Confidence map, (b) binary map, (c) peak position estimation.

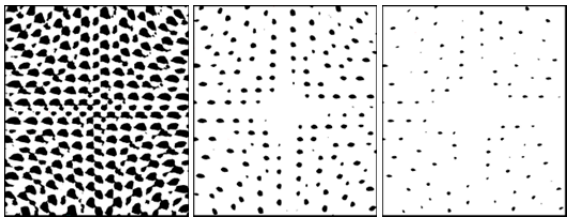

Figure 7: Peak selection with too low (a), correct (b), and too high (c) threshold.

The key part of the extraction method is the threshold level selection. An illustrative example is shown in Figure 7, with peaks selected with too low, correct, and too high thresholds. In the case of low threshold value the separate regions are merging (see Figure 7(a))), while the too high threshold value causes lower number of detected peaks (see Figure 7(b)). In real cases the confidence values highly depend on the measurement noise and vary in each measurement round. Thus a constant threshold values, as in Figure 5(a), should be avoided.

The proposed dynamic threshold value selection (shown on Figure 5(b)) is based on the histogram of the confidence map. A typical histogram and cumulative histogram can be seen in Figure 8(a) and Figure 8(b), respectively. The dynamic threshold value is determined as the value where 90% of the confidence map values are lower than the selected value, as shown in Figure 8.

3.2 Confidence Map-based Peak Prediction

The proposed peak prediction method enhances the tracking robustness by predicting the peaks' movements based on the confidence map itself. There are time instances where the confidence value of a possible position can go below the threshold value as can be seen on Figure 5(b), which makes

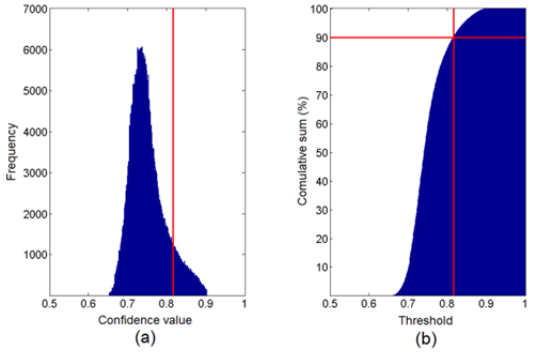

Figure 8: Typical (a) histogram and (b) cumulative histogram of a confidence map. Red lines show the selected threshold value.

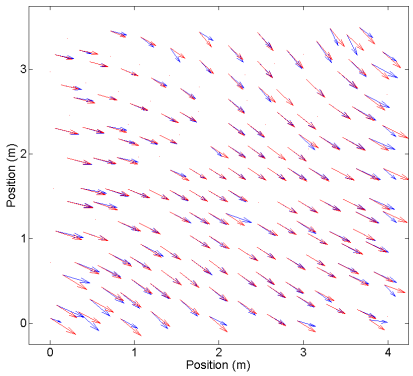

Figure 9: Illustration of the predictive peak tracking. Blue arrows show the calculated (true) movement vectors of the peaks in one iteration, red arrows show the predictions for the same vectors. For better visibility the vectors were enlarged.

the associated track impossible to follow. The original algorithm presented in (Zachár, 2014) marks the track as dead and stops tracking the real or phantom object positions in these cases.

In the proposed solution uses three track attributes: alive, alive but invalid, and dead. Alive tracks become invalid, when the peak is lost, but kept alive for a limited number of measurement rounds. For invalid tracks the position is estimated from the last known or estimated position (i.e. peak location).

The proposed solution focuses on solving the recovery problem; making the tracks alive for a longer period and assign them to the appropriate possible position. The key idea can be seen in Figure 9; possible positions of a peak can be estimated in consecutive measurement rounds using the confidence map. The displacement of a lost peak can estimated from the displacement of other peaks in the close vicinity. This idea is illustrated and also justified the by Figure 9, where the movement vectors, calculated from a real measurement, are approximately the same in a small neighborhood. Thus the proposed solution predicts the displacement of a given point P as follows:

$$\overrightarrow{P_{pred}} = \frac{\sum_{k=1}^{n} \overrightarrow{A_k B_k}}{n}, \left\| \overrightarrow{PA_k} \right\| < L \qquad (5)$$

where A_k and B_k are the initial and the end points of a nearby movement vector, calculated from two consecutive confidence maps, and n is the number of vectors within a specified distance L.

3.3 Tracking Algorithm

The pseudo-code of the tracking algorithm is shown

```
 1 input: phases(k), k=1..n
 2 output: aTrack, iTrack, dTrack

 3 function TrackPositions

 4 aTrack = {}
 5 fTrack = {}
 6 dTrack = {}

 7 map = genConfidenceMap(phases(1))
 8 points = possiblePositions(map)
 9 for each p ∈ points
10   t= new Track
11   t.add(p)
12   aTrack = aTrack ∪ t
13 endfor

14 for each ph ∈ phases(2..n)
15   prevPoints = points
16   map = genConfidenceMap(ph)
17   points = possiblePositions(map)

18   ap1 = assignPoints(prev_points,
          points, ACTIVE_LEVELS)

19   usedPoints = {};
20   newATrack = {};
21   newITrack = {};
22   for each t ∈ aTrack
23     if isAssigned(ap1, t.last)
24       p = getNewPoint(ap1, t.last)
25       t.add(p)
26       t.invalid = 0
27       usedPoints = usedPoints ∪ p
28       newAtrack = newAtrack ∪ t
29     else
30       p = predict(ap1, t.last)
31       t.add(p)
32       t.invalid = 1
33       newITrack = newITrack ∪ t
34     endif
35   endfor

36   iTPos = collectPoints(iTrack)

37   ap2 = assignPoints(iTPos,
        points\usedPoints, PREDICT_LEVELS)

38   for each t ∈ iTrack
39     if isAssigned(ap2, t.last)
40       p = getNewPoint(ap2, t.last)
41       t.add(p)
42       t.invalid = 0
43       newATrack = newATrack ∪ t
44     else
45       p = predict(ap1, t.last)
46       t.add(p)
47       t.invalid = t.invalid + 1
48       newITrack = newITrack ∪ t
49     endif
50   endfor

51   dTrack = selectDead(newITrack,Ndead)
52   iTrack = newITrack \ dTrack
53   aTrack = newATrack

54 endfor
```

Figure 10: Pseudo code of the prediction-aided tracking algorithm.

in Figure 10. The input of the proposed tracking algorithm in each time instant k ($k = 1, 2, \ldots, N$) is the measured phase vector $\vartheta_{meas}(k)$. The vector length varies depending on the on the number of the utilized configurations (see Figure 2). The outputs of the algorithm are the lists of active, inactive and dead tracks; *aTrack*, *iTrack*, *dTrack* respectively (see lines 1-2). Ideally the active tracks list contains only one element which belongs to the real object movement. At the beginning of the algorithm new tracks are created for each of the possible positions, containing the real object position and several phantom positions (lines 4-13). In each of the following measurements rounds the new possible positions are calculated and the movements of the tracks are computed (lines 14-54). First the new confidence map is calculated and the peak positions are identified (lines 15-18). Then each active track is checked whether a detected peak can be regarded as the follow-up of the track (line 23). If a track can be followed then it will be marked as active and the measured new position is used as the last position of the track (lines 24-28). If a track cannot be followed (due to a lost peak) then the new position will be predicted and the track will be marked as inactive (lines 30-33). Inactive tracks are similarly handled in lines 37-50. At the end of the iteration the dead tracks are separated from the inactive tracks (lines 51-53). The current solution marks a track dead if it is inactive for N_{dead} consecutive iterations.

4 EVALUATION

The performance of the proposed algorithm was tested with real measurements. In the test four infrastructure nodes and one tracked node were used. The algorithm utilized all the twelve possible configurations *C1-12* (see Figure 2). The test was performed in a 4.5 m by 4.5 m room where the infrastructure nodes were placed in the corners of a 3 m by 3.5 m rectangle, 2 m above the ground level (at coordinates (0, 0, 2), (0, 3, 2), (3.5, 0, 2), and (3.5, 3, 2) in Figure 11). The moving node was

carried in hand by a person (probably causing small deviations in the range of a few dozens of millimeters). The tracking results of the proposed algorithm can be seen in Figure 11, where phantom and real tracks are shown in blue and red, respectively. With no prediction (Figure 11(a)) the tracking failed after a few seconds because of noisy measurements. With the same measurement data the proposed algorithm performed well and was able to follow the movement, since the missing estimates were successfully replaced by predictions (see Figure 11(b)). In the test the parameter N_{dead} was set to five.

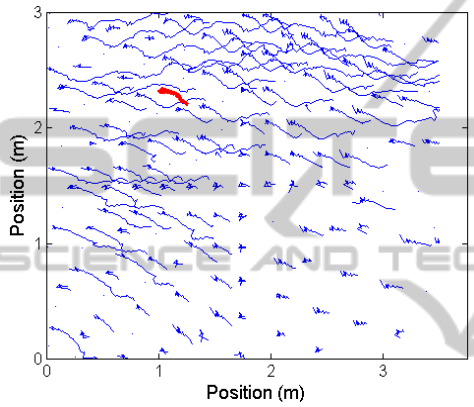

(a)

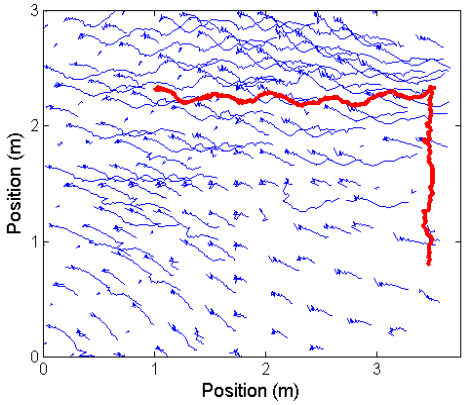

(b)

Figure 11: Tracking results of the measurement (a) without and (b) with peak prediction.

Figure 12 shows the reference trajectory in magenta and the estimated true trajectory. The maximum deviation from the reference track is 91 mm, part of which is probably caused by the carrying person.

The estimated and predicted values in Figure 12 are shown in blue and red, respectively. It is interesting to note that at the magnified part of the track the predictions follow very well the true estimated trajectory, despite of the fact that the

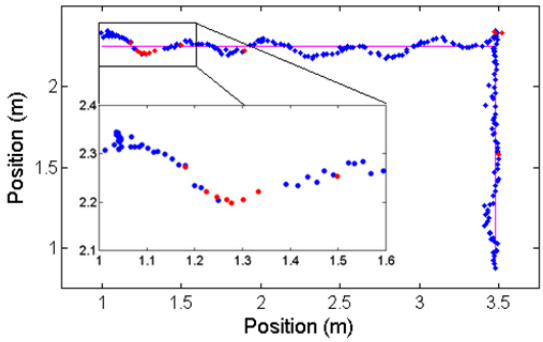

Figure 12: The longest track of the measurement. The estimated and predicted positions are shown with blue and red dots, respectively. The true track is shown in magenta.

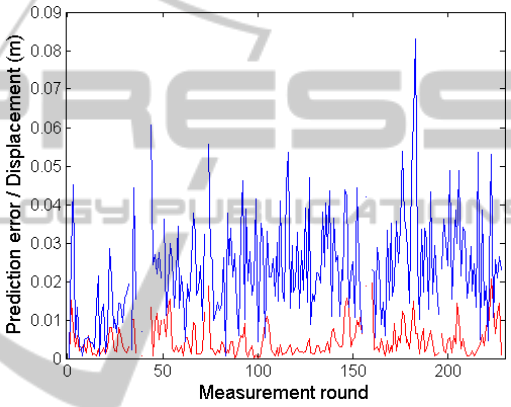

Figure 13: Prediction error (red values) and the lengths of displacement vectors (blue values) of the real object track.

trajectory changed its direction while only the predicted values were available. Such prediction, based on models on the movement itself, would be very troublesome, but the proposed prediction scheme using the peaks in the neighborhood handles the situation properly.

The behavior of the tracking system is illustrated in Figure 13, where the distances between the consecutive position estimates are plotted in blue (missing estimates, shown in red in Figure 12 are omitted here). The average displacement is 0.023 m, corresponding to an object speed of approximately 0.25 m/s. The quality of the proposed prediction scheme is also evaluated in Figure 13. The true track of the previous measurement (plotted in blue in Figure 12) was used as reference, and in each iteration the predicted positions were also calculated and compared to the estimated positions. The difference is shown in red in Figure 13. The average prediction error is 5 mm, while the maximum error was 21 mm. Clearly the proposed prediction scheme is able to accurately replace the estimates when they are not available.

The experimental results show that the proposed method is capable of tracking a moving object equipped with a sensor node device. In contrast to RIPS (Maroti, 2005) or SRIPS (Dil, 2011), the proposed tracking algorithm utilizes only one measurement frequency, resulting shorter measurement times for each measurement round. Thus the phase difference measurement errors, caused by the object movement, can be minimized and the proposed method is able to provide a robust tracking, while preserving the few centimeters of accuracy of the interferometric-based localization techniques.

5 CONCLUSIONS

In this paper a novel object tracking method was proposed, which utilizes radio-interferometric phase measurements and confidence maps. The presented solution enhances the robustness and quality of the position estimations when bad measurements are present or measurements are temporarily missing, using (1) a new peak detection method utilizing a dynamic threshold, and (2) by a novel prediction method, which is able to substitute missing estimates with predicted positions. The proposed prediction method examines the evolution of the confidence map in time and calculates the predicted position from it, without any external model on the movement of the tracked object.

The complexity of the proposed algorithm is moderate thus it can be implemented in real time using ordinary computers.

The performance of the proposed algorithm was illustrated and evaluated by real measurements. The proposed prediction method was validated: the mean prediction error was typically 5 mm, while the maximum error was 21 mm during the experiment. The increased robustness of the algorithm was clearly shown in the experiments where the proposed algorithm was able to follow the object movement with maximum error of 91 mm, despite of the measurement noise and errors.

ACKNOWLEDGEMENTS

This work was partially supported by the Hungarian State and the European Union under project TAMOP-4.2.2.-C-11/1/KONV- 2012-0004.

REFERENCES

Au, A.W.S., et al, 2012. Indoor Tracking and Navigation Using Received Signal Strength and Compressive Sensing on a Mobile Device. *IEEE Transactions on Mobile Computing*, Vol. 12, No. 10, pp. 2050–2062.

Dil B.J., Havinga, P.J.M., 2011. Stochastic Radio Interferometric Positioning in the 2.4 GHz Range. *Proceedings of the 9th ACM Conference on Embedded Networked Sensor Systems (SenSys 11)*, Seattle, WA, pp. 108-120.

Kai Ni, Kannan, A., Criminisi, A., Winn, J., 2009. Epitomic Location Recognition. *IEEE Transactions on Pattern Analysis and Machine Intelligence*, Vol.31, No.12, pp. 2158-2167.

Lanzisera, S., Zats, D., Pister, K. S. J., 2011. Radio Frequency Time-of-Flight Distance Measurement for Low-Cost Wireless Sensor Localization. *IEEE Sensors Journal*, Vol. 11, No. 3, pp.837-845.

Maroti M., et al, 2005. Radio Interferometric Geolocation. In *ACM Third International Conference on Embedded Networked Sensor Systems (SenSys 05)*, San Diego, CA, pp. 1-12.

Mulloni, A., Wagner, D., Barakonyi, I., Schmalstieg,D., 2009. Indoor Positioning and Navigation with Camera Phones, *IEEE Pervasive Computing*, Vol. 8, No. 2, pp. 22-31.

Peng, C., Shen, G., Zhang, Y., Li, Y., Tan, K., 2007. BeepBeep: a high accuracy acoustic ranging system using COTS mobile devices. In *Proceedings of the 5th international conference on Embedded networked sensor systems* pp. 1-14.

Se, S., Lowe, D., Little, J., 2001. Vision-based mobile robot localization and mapping using scale-invariant features. *Proceedings of 2001 IEEE International Conference on Robotics and Automation*, Vol.2, pp. 2051-2058.

Zachár, G., Simon, G., 2014. Radio-Interferometric Object Trajectory Estimation. *Proc. 3rd International Conference on Sensor Networks, SENSORNETS 2014*, pp. 268-273.